Multi-Voltage Level Active Distribution Network With Large Share of Weather-Dependent Generation

Aeishwarya Baviskar ⓘ, *Student Member, IEEE*, Kaushik Das ⓘ, *Senior Member, IEEE*, Matti Koivisto ⓘ, *Member, IEEE*, and Anca Daniela Hansen ⓘ, *Member, IEEE*

Abstract—Utility-scale and small scale wind and solar power installations along with electric vehicle charging stations, and other active sources of energy are increasing at the medium and lower voltage levels in the distribution grid. This situation requires a better understanding of the impact of high penetration of weather-dependent renewable energy sources on the operating conditions of the distribution network at both medium and low voltage levels. Despite the need, a multi-voltage level distribution network model, based on real network data and weather-dependent renewable generation data, has not been presented for distribution grid studies. This paper presents a comprehensive multi-voltage level active distribution network model based on real network data along with load and generation time-series for about a year. The network topology is modelled based on geographical data for various rural, semi-urban, and urban locations. The distribution network is embodied with a large share of renewable generation sources, with generation time-series simulated from meteorological data. The network is also flexible to incorporate other assets such as electric vehicle charging stations, storage, etc. The presented active distribution network model can be used to study, optimize, and control the effects of weather-dependent generation and other network assets in the distribution grid.

Index Terms—Active distribution network, generation profile, load profile, network assets, network topology, renewable generation.

I. INTRODUCTION

DISTRIBUTED Renewable Energy Sources (RES), including utility-scale installations and small-scale projects closer to the point of consumption, have a major role to fulfill the ambitious renewable energy targets set by various countries. Distributed RES are also crucial in providing access to energy in developing and under-developed economies around the world. Feed-in tariff programs and financial support schemes were key drivers to increase the share of renewable energy sources in the grid [1,2,3]. In recent years, declining electricity cost via renewable energy sources and growing interest in self-consumption have boosted the distributed renewable energy markets in Europe as well as the world [4]. Weather-dependent energy sources, like solar photovoltaics (PV) and wind power plants (WPP), are at the forefront, accounting for a large share in utility-scale, commercial, and user-end installations [4]. Furthermore, storage units, electric vehicle (EV) charging stations, combined heat power plants are gaining increasing popularity, and have the potential to become an integral part of the future distribution grid. Thus, a future distribution network resembles more closely an active network with multiple assets such as weather-dependent generation, combined heat cycle plants, electric vehicle charging, etc. There is, however, a growing concern among distribution system operators (DSOs) for loss of revenue, increased operation cost, and the threat of disintermediation [6, 7].

The main hurdle behind the cost-effective operation of distribution network with a large share of weather-dependent RES is due to their intermittent/fluctuating and non-dispatchable nature as discussed in [1]–[3]. Additionally, these assets are connected at different voltage levels (owing to the power carrying capabilities of different voltage levels and installation size). Advanced power electronics converters in these assets render them controllable. When the assets are controlled in each of these different voltage levels, the change in power flows not only impact that specific voltage level but also other voltage levels too in terms of voltage profile, power losses, reactive power flow, etc. This has a further impact on the active and reactive power flow to the transmission network. It is thus necessary to study, analyze, and develop active management techniques for the growing number of beneficial network assets connected in the distribution grid. As a result, a benchmark distribution network model representing the characteristics of a large share of integrated generations in each voltage level is of particular interest.

The design of benchmark models in power systems has been a topic of interest for many research works. A brief summary of some network models is presented in Table I The benchmark models presented by the CIGRE Task force are one the most commonly used and well known distribution network benchmark models. The CIGRE Task Force developed distinct high, medium and low voltage benchmark networks for studying and analyzing network behavior in presence of distributed energy

TABLE I
SUMMARY OF A FEW OPEN-SOURCE DISTRIBUTION NETWORK MODELS

	Application	Voltage level	Network Topology	Time-series
[4]	Power Flow analysis	Distribution;	Synthetic	-
[11]	Congestion management, transmission capacity, grid stability, etc.	Transmission	German: from geographical data	-
[12]	open source planning platform	Distribution; unbalanced	Synthetic	1 hour resolution for 1 year
[8]	Quasi-steady state time-series solutions, smart grid studies	All	USA; Synthetic	Taxonomy models representing different days
[13]	Power Flow analysis	Transmission and Distribution	German; Partly synthetic	15 min resolution for 1 year
[7]	Testing new algorithms, and distribution system elements	Distribution; unbalanced	USA & Europe: Synthetic	One minute resolution for 24 hours
[14]	developing control and optimization algorithms for active management in distribution grid	Distribution; Multi-voltage; Balanced	Denmark; from Geographical data	One hour resolution for 10 months

sources including RES [4]–[6]. However, the network topology for the CIGRE models does not represent a real distribution network. Another set of benchmark models that demand noteworthy attention are the IEEE distribution network models [7]. The IEEE distribution feeders were developed with multiple objectives such as testing new algorithms or distribution system elements such as transformers in unbalanced networks. The IEEE distribution feeders do not focus on high share of renewable generation. In addition, only 24 hours of load time-series data is available with the IEEE distribution feeders and most of the networks are synthetic, except for the 8500 IEEE distribution feeder. GridLAB-D is an open source transmission and distribution grid simulation environment with taxonomic load time-series data for different scenarios [8] developed especially to study quasi steady state operations and smart-grid applications. Furthermore, to address the overestimates of grid extension needed due to increasing distributed energy sources and storage installations in transmission and distribution networks, synthetic open-source medium voltage distribution networks, called the *eGo grid models* are presented in [9]. Another example of grid models studying RES and other low-carbon technologies arr the *Low Voltage Network Models and Low Carbon Technology Profiles* founded on the U.K. distribution network [10]. It emphasizes the growing interest in analyzing distribution network behavior pertaining to the aforementioned developments.

Some network models have been developed recently with the help of open source geographical data such as *Open Street Maps* [15] which represents a real distribution network more closely than synthetic models. Works addressing generation or synthesis of benchmark models can be found in [9], [16]–[18]. *SciGRID* is an example of open source network model intended towards studying congestion management, transmission capacity, grid stability in the transmission networks developed on data from *Open Street Maps* [11].

SimBench is one of the more recent additions to the library of open-source benchmark models developed on principles presented in [13], [17]. The grid data in *SimBench* is in accordance with the German Distribution System Operator (DSO)'s operation and planning principle with partly synthetic network topology. Furthermore, *SimBench* also provides load time-series for about one year for different types of consumer behavior.

More often the network topology in the open-source models is based on synthetic network modeling. Amongst all the distribution network models presented so far, there are two multi-voltage network models which include the low voltage levels [13], [18] and only [12], [13] is accompanied with load time-series data for over a year. However, to study the effect of weather-dependent generation in a future active distribution grid, it is crucial to also study the correlation between the load demand and weather-dependent generation at different voltage levels in the network. Thus, a real distribution grid model with focus on load time-series and correlated weather dependent generation time-series, and the ability to incorporate with modern network assets such as storage, EV charging, combined heat plants, etc. is lacking. In this respect, this research proposes and presents such a multi-voltage level distribution network model, which is needed for an exhaustive study of the performance, operation and control of future weather-dependent distribution networks.

The proposed distribution network model, is an open source network model, entitled as the *DTU 7 k Bus Active Distribution Network* (DTU-ADN), is accompanied by load time-series aggregated at 60 kV, 10 kV and 0.4 kV. The network topology for the DTU-ADN is generated from geographical data and represents real distribution networks. The objective behind the development of the DTU-ADN is the development of control and optimization algorithms for active management of future distribution network with aforementioned assets.

Some novel features of the proposed and developed benchmark distribution network model are as following:

- Weather-dependent generation time-series simulated from meteorological data and correlated load time-series, derived from measurement data at three different voltage levels
- Capability to co-simulate a multi-voltage distribution network with large share of RES at different voltage levels to evaluate impact of distributed generation on the operational conditions of a distribution network
- 18 different realistic and diverse network topology of 10 kV-0.4 kV networks with different characteristic loads, such as agricultural, household, and/or industrial, and distributed RES

- Flexibility to incorporate additional network assets such as combined heat and power plants, storage units, electric vehicle charging stations, etc. to investigate performance of active distribution networks
- Comprehensive platform for development of coordinated control between different assets for optimal operation of distribution network, while incorporating uncertainty from weather dependent generation and loads.

Section II briefly introduces the *DTU 7 k Bus Active Distribution Network* along with the publicly available data for the network. The raw data used to develop the distribution network model and methodology is described in Section III. Results of the implemented methodology are presented in Sections IV, and V summarizes the presented active distribution grid model and the research methodology by highlighting its crux.

II. DTU 7k-Bus Active Distribution Network

The DTU 7k-Bus Active Distribution Network (DTU-ADN) [14] is a balanced three-phase multi-voltage network with a high share of weather-dependent renewable energy generation. The complete dataset for DTU-ADN is open-source. It spans across three voltage levels, 60 kV-10 kV-0.4 kV, while being connected to the transmission grid via step-up 60 kV/150 kV transformers. The medium voltage (MV) 60 kV network can be connected to 17 distinct 10 kV-0.4 kV networks, simultaneously or in combinations, at different 60 kV-10 kV substations, to form a three voltage level network. This section presents key features of the DTU 7k-Bus Active Distribution Network.

A. The 60 kV Network

The topology of the 60 kV network originates from a real Danish grid. It hosts 25 buses out of which 23 buses connect 60 kV/10 kV substations, and one bus connects to the transmission grid via 60 kV-150 kV step-up transformers. On-load tap changers are present at the 60 kV-150 kV transformer and also at the 60 kV-10 kV substation transformers. The 60 kV network hosts three WPPs with installed capacities of 12MW, 15MW, and 15MW composed of type IV controllable wind turbines. Fig. 1 illustrates the network topology with its key elements.

Measurement data in a real distribution network, based on historical data for 1 a, forms the basis of the load (active and reactive power) and generation time series accompanying the 60 kV grid. Aggregated load time series at all the 60 kV/10 kV substations, and generation time series for the three WPPs are provided for the 60 kV network. As a consequence of a large share of distributed generation, negative values, or reverse power flow is also observed in the aggregated load time series at the 60 kV–150 kV and 60 kV/10 kV substations.

B. 10 kV-0.4 kV Networks

Topology for the 10 kV-0.4 kV networks associated with the DTU-ADN represents unique layouts as they are derived from publicly available data from *open street maps* [15] using Distribution Network Models module (DiNeMo) [19]. The networks
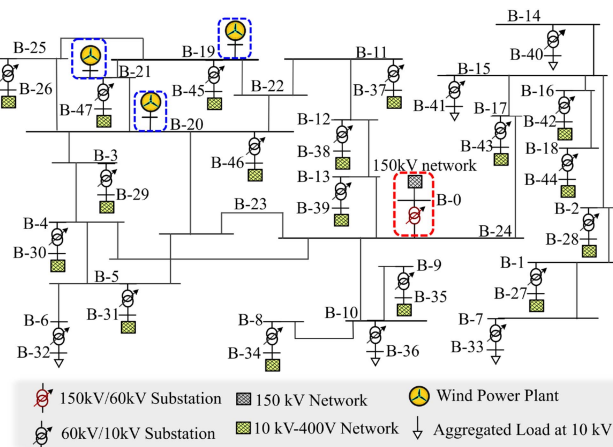

Fig. 1. Network topology for the 60 kV network in the DTU 7k-Bus Active Distribution Network indicating locations of the Wind Power Plants, and 10 kV-0.4 kV networks.

cover varied geographical areas, thus making some networks dense, akin to urban networks, and others more sparse, comparable to rural networks. The number of supply or generation nodes in the networks falls in the range of 40 to 650 nodes. Cumulatively, the entire DTU-ADN consists of approximately 6541 nodes at 0.4 kV, 427 nodes at 10 kV, and 25 nodes at 60 kV which accounts for its name DTU 7k-Bus Active Distribution Network. In addition, there are a total of 291 10 kV/0.4 kV substations with off-load tap changing transformers within the 10 kV 0.4 kV networks.

The DTU-ADN dataset also specifies unique load profiles for each of the 10 kV-0.4 kV nodes. Since, the DTU-ADN is a balanced three-phase distribution network model, the 10 kV, and 0.4 kV nodes serve multiple customers connected to these nodes, thus the load and generation time series mirror aggregated values. The load time series provided with the dataset are categorized into four main categories, namely household, industrial including commercial, agricultural, and miscellaneous loads. In total there are 27 different load time series derived from [17]. All the 10 kV-0.4 kV networks have varied proportions of load profiles from each category. Thus, the 10 kV-0.4 kV networks can be further classified in terms of their cumulative maximum load demand from each category into predominantly residential networks, highly industrialized networks, or agricultural networks.

Fig. 2 shows an example of one of the 10 kV-0.4 kV networks at Bus 27. Fig. 2 indicates the network topology, with the distribution lines, and all the nodes with specified load profile category.

C. Weather-Dependent Generation

Numerous nodes in the 10 kV-0.4 kV networks have either solar or wind or both generation sources installed along with the load. The assortment of installed solar capacities is from a minimum of a few kWs to approximately 2.5MW. Similarly, installed wind capacities range from a minimum of $300kW$ to a maximum of $16MW$. The cumulative installed solar and
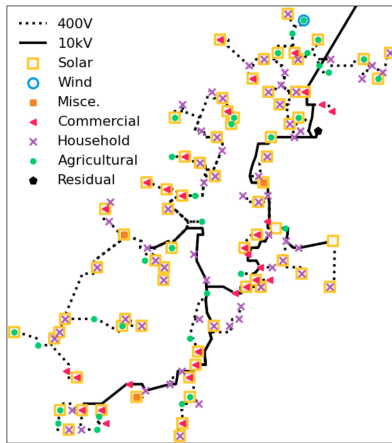
Fig. 2. The 10 kV-400 V network at Bus 27 illustrating 10 kV and 0.4 kV distribution lines, type of load profiles at each node, location of solar and wind power installations.

TABLE II
OPTIMIZATION RESULT BEFORE AND AFTER DYNAMIC TIME-WARPING FOR
10 KV-0.4 KV NETWORKS AT BUS 27, 28 AND 46

Network at Bus	Without DTW		With DTW	
	RMSE*	Correlation	RMSE*	Correlation
27	0.31	0.7818	0.28	0.825
28	0.27	0.71	0.15	0.92
46	2.932	0.908	2.8	0.91

wind capacities in the DTU-ADN are approximately $26MW$ and $150MW$ respectively.

There are approximately 1900 distributed generators across the 10 kV-0.4 kV networks, amongst which about 300 installations across 17 networks can actively participate in the grid operations via advanced power electronics control. The distinction between passive and actively participating distributed generation is made according to the Danish grid codes and may vary depending on the local grid codes. The presence of smaller distributed generation units $(< 11kW)$ along with the controllable units account for their different effects on distribution grid operations due to their uncontrollable and controllable properties.

For Network at Bus 27, the installed solar capacity is 1.85 MW which is distributed amongst numerous nodes, and the wind capacity is 0.44 MW at a single node (See Fig. 2).

D. Possible Applications

The DTU-ADN data set can be used to analyze the effect of a high share of renewable energy in rural, semi-urban, or urban network topology. It can extended to analyze the diurnal, seasonal, weather and temperature dependent effects on the active and reactive power demand, voltage profiles, power losses, etc. from a distribution network using the time-series data provided with the network dataset. Furthermore, effect on distribution network assets, such as on-load tap changers, voltage regulators, switching capacitors, can be studied in presence of a highly weather-dependent power flow.

The DTU-ADN can be used as a platform to study various control strategies at medium or low voltage levels and analyze their effects on the overall performance of the network with correlated load and weather-dependent generation. It provides a unique opportunity to investigate the long term effects of actively controlling large number of distributed renewable generation in local network operations of a distribution network as well as the interaction between transmission and distribution networks. In addition, the network model is flexible to incorporate storage, electric vehicles, combined heat plants, hybrid power plants

etc. at the distribution level. This enhances and expands its applicability to multiple study areas.

E. How to Access the Data?

The DTU-ADN is an open-source dataset available in an online repository [14]. The dataset in the repository is the first version of the DTU 7k-Bus Active Distribution Network and is subject to updates as the work progresses. All the network files in the dataset are *csv* files suitable to be directly used in MatPower, PandaPower or Pypower. Further description of the data can be found in the readme file included.

III. NETWORK MODELING METHODOLOGY

This section describes the methodology used to generate the DTU 7k-Bus Active Distribution Network (DTU-ADN). The first sub-section presents the raw data used in DTU-ADN model generation. The second sub-section outlines an optimization algorithm, which decomposes the aggregated 60 kV load-generation profile into individual 10 kV or 0.4 kV load-generation profiles. The final sub-section describes a heuristic algorithm used to assign load-generation profiles to individual 10 kV or 0.4 kV nodes.

A. Raw Data

1) 60 kV Network: The network topology, line, and transformer data for the 60 kV network serves as a good representatives of a real network as it is derived from a real distribution network. The aggregated load time-series at 10 kV and the WPP generation data is derived from measurement data from this network.

2) 10 kV Network Topology: To generate a 10 kV-0.4 kV network DiNeMo takes as input an area of interest from *Open Street Map* and reproduces a representative distribution grid [15], [19]. Additional inputs include an approximate geographical location of the 60 kV / 10 kV substations from Fig. 1, population / consumer density, probability of consumers per building [%], Minimum low voltage demand [kW], Minimum MV demand [kW], Voltage level [kV], and transformer capacity for the location. The National Denmark statistical data provides inputs to generate realistic 10 kV-0.4 kV networks in terms of energy consumption patterns and load distribution. Thus, the DTU-ADN represents a set of realistic and diverse networks in terms load distribution, consumption and network topology as highlighted through the example networks presented in Table III.

The 10 kV–0.4 kV network generated by DiNeMo includes distribution line data, MV/LV substation data, switches in the network, and approximate value of the load at each node. The

TABLE III
STATISTICS FOR 10 kV-0.4 kV NETWORKS AT BUS 27, 28 AND 46

Network at Bus	27	28	46
Type of network	rural	semi-urban	urban
No. of Nodes at 10 kV	8	15	31
No. of Nodes at 0.4 kV	134	270	494
Max. load*	3.51	2.6	2.77
Min. load*	0.26	0.41	-24.73
Max. Household load*	1.95	0.52	2.75
Max. Agricultural load*	1.75	1.35	0
Max. Commercial/Industrial load*	1.82	1.85	1.88
Installed PV capacity*	1.85	0.57	3.4
Installed WPP capacity*	0.44	0	36.5

load data from DiNeMo lists a demand in *kVA* for each node based on the maximum demand input provided at the time of network generation. The demand in *kVA* provided by DiNeMo is then used to scale and assign Standard Load Profile (SLP)s at every node in the network.

3) Standard Load Profiles: The SLPs provided by Sim-Bench [20] are used in this work to derive load time-series for individual 0.4 kV and 10 kV nodes.

4) Wind and Photovoltaic generation profiles: The wind power generation profiles and photovoltaic profiles provided with the data set are generated using the DTU Correlations in Renewable Energy Sources (CorRES) simulation tool using meteorological time-series and stochastic simulations [21].

Geographical location of the PV plant, installed capacity [MW], surface azimuth angle and surface tilt are the input to CorRES to generate PV generation profiles for the given time. Global Solar Atlas provides inputs for the surface azimuth angle and tilt for the chosen geographical location [22]. Since, the geographical span of the 10 kV-0.4 kV networks is constrained to a small area, a uniform PV output is assumed throughout each 10 kV-0.4 kV network and only one PV profile is generated per 10 kV-0.4 kV network.

The data register for WPPs provides a comprehensive list of WPP installations across Denmark along with their hub heights, installed capacities, number of turbines, turbine rated power, turbine diameter, etc. [23] The input data for simulating WPP's generation profile in CorRES is thus directly taken from the data register [23]. WPPs located geographically closer to the 60 kV/10 kV substation are chosen for simulation. Thus, there may be multiple WPP generation profile associated with a 10 kV/0.4 kV network.

B. Optimization Algorithm

The optimization aims to break down the load time-series aggregated at 10 kV into a weighted sum of SLPs and weather-dependent generation profiles as shown in Fig. 3. The residual time-series in Fig. 3 refers to a characteristic component of the load time-series aggregated at 10 kV which cannot be encapsulated via individual or combination of any available SLP and generation time-series. The optimization is performed individually for each of the 10 kV-0.4 kV networks.

Let $\mathcal{L}$ be the set of all available SLPs and $\mathcal{W}$ be the set of all weather-dependent generation profiles available for one 10 kV-0.4 kV network. $\mathcal{R}$ is the set of real numbers and $\mathcal{Z}$ is
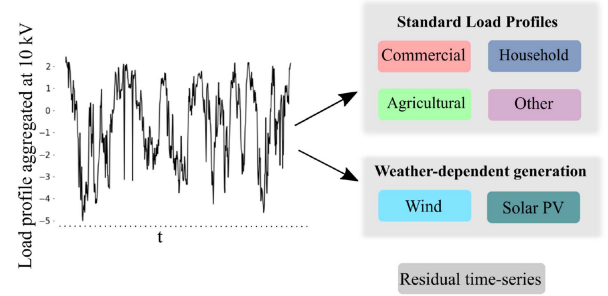

Fig. 3. Breakdown for load time-series aggregated at 10 kV into weighted sum of standard load profiles, weather-dependent generation, and the residual time-series.
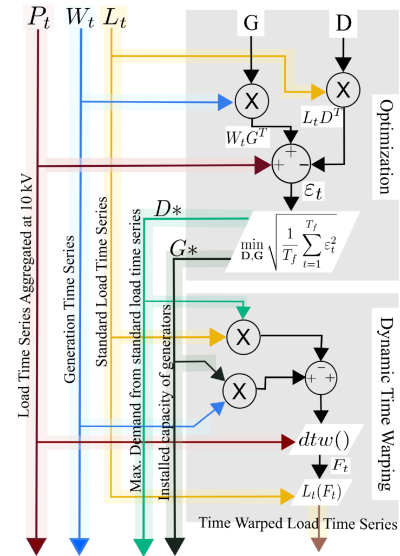

Fig. 4. Flowchart depicting the input and output data from the optimization algorithm and dynamic time warping process.

the set of integers. The following notations are defined for the optimization algorithm,

- P_t: load aggregated at 10 kV, at time t in MW
- $\mathbf{L}_t$: vector containing load from all SLPs at time t in $p.u.$
- $l_{i,t}$: power demand for the ith SLP at time t in $p.u.$, where $i \in \mathcal{L}$
- $\mathbf{W}_t$: vector with weather dependent generation in $p.u.$
- $w_{j,t}$: generation from the jth generation profile at time t in $p.u.$, where $j \in \mathcal{W}$
- $\mathbf{D}$: vector containing maximum load from all the SLPs in MW
- d_i: maximum load for the ith SLP in MW, where $i \in \mathcal{L}$
- $\mathbf{G}$ vector containing installed generation capacity for all available generation profiles for a particular 10 kV-0.4 kV network in MW
- g_j: installed generation capacity from the jth generation profile in MW, $j \in \mathcal{W}$

The data flow in the optimization algorithm and dynamic time warping process is depicted in Fig. 4 . Load time-series

aggregated at 10 kV (P_t), SLP load vector ($\mathbf{L}_t$), and weather-dependent generation vector $\mathbf{W}_t$ are the inputs to the optimization. The outputs from the optimization are the maximum load vector for each SLPs (**D**), and a vector containing installed generation capacity of PV and wind in the network (**G**). The dynamic time warping process is explained in the following section.

$\mathbf{L}_t$, a vector of load for all SLPs, in $p.u.$, at time t, can be written as,

$$\mathbf{L}_t = \begin{bmatrix} l_{1,t} \ l_{2,t} \ \dot{s} \ l_{27,t} \end{bmatrix} \tag{1}$$

$\mathbf{W}_t$, a vector with weather-dependent generation, in $p.u.$, at time t, can be written as

$$\mathbf{W}_t = \begin{bmatrix} w_{1,t} \ w_{2,t} \ \dot{s} \ w_{k,t} \end{bmatrix}, k \in \mathcal{Z}. \tag{2}$$

Vector with cumulative maximum demand for all SLPs, **D**, can be written as,

$$\mathbf{D} = \begin{bmatrix} d_1 \ d_2 \ \dot{s} \ d_{27} \end{bmatrix} \tag{3}$$

and vector **G** containing the maximum weather-dependent generation for solar and wind profiles, is written as,

$$\mathbf{G} = \begin{bmatrix} g_1 \ g_2 \ \dot{s} \ g_k \end{bmatrix}, k \in \mathcal{Z}. \tag{4}$$

Let ε_t denote the difference between load profile aggregated at 10 kV and weighted sum of SLPs and weather-dependent generation, at time t, representing the residual time-series,

$$\varepsilon_t = P_t + \mathbf{W}_t\mathbf{G}^T - \mathbf{L}_t\mathbf{D}^T. \tag{5}$$

It is assumed that all the 10 kV-0.4 kV networks have local generation sources. The local generation in the network is accounted by adding the weighted generation time series, $\mathbf{W}_t\mathbf{G}^T$, to the load time-series aggregated at 10 kV, P_t. Thus, weighted sum of the SLPs, $\mathbf{L}_t\mathbf{D}^T$, represents the load in the network in correlation with the local generation. The objective of the optimization is to reduce the residual time-series by minimizing root mean square error of ε_t,

$$\min_{\mathbf{D},\mathbf{G}} \sqrt{\frac{1}{T_f} \sum_{t=1}^{T_f} \varepsilon_t^2} \tag{6}$$

where T_f is the length of the available time-series. The variables for the optimization algorithm, **D** and **G**, are unconstrained and unbounded. The optimization algorithm is thus a linear programming problem which is solved in *Python* using *CPLEX*.

The load profile aggregated at 10 kV is derived from measurement data in Denmark for the year 2014-15, while the available SLPs originate from a German distribution grid from the year 2016. Load profiles are decidedly dependent on weather and user behavior at the time of day. Hence, the load profile aggregated at 10 kV and SLPs have temporal dissimilarities, which explain the presence of a residual time-series. However, the temporal dissimilarities can be further reduced by time warping the German SLPs according to the 10 kV aggregated load profile.

Dynamic Time Warping (DTW) was initially applied as a pattern matching algorithm wherein the time-axis fluctuation is modeled with a nonlinear time warping function by [24], [25]. The time warping function is then applied to eliminate time differences between two signals for maximum coincidence. The problem is drafted as a dynamic programming problem, with the time-warping function being the optimization variable.

DTW is used to reduce temporal mismatch between the weighted sum of SLPs and the aggregated load time-series at 10 kV while incorporating the presence of weather-dependent generation in the 10 kV-0.4 kV network. DTW generates a time warping vector $\mathbf{F}_t$ given the following inputs,

$$\mathbf{F}_t = dtw(P_t, \ \mathbf{L}_t\mathbf{D}^T - \mathbf{W}_t\mathbf{G}^T). \tag{7}$$

The time-warping vector is then used to warp the SLP time-series vector, $\mathbf{L}_t$. Let the time warped SLP vector be termed H_t,

$$\mathbf{H}_t = \mathbf{L}_t(\mathbf{F_t}) \tag{8}$$

$$\mathbf{H}_t = \begin{bmatrix} h_{1,t} \ h_{2,t} \ \dot{s} \ h_{27,t} \end{bmatrix}$$

where $h_{i,t}, i \in \mathcal{L}$ is the load from the ith time warped load profile for a particular 10 kV-0.4 kV network.

Since, the optimization and dynamic time warping is performed individually for all the 10 kV 0.4 kV networks, the load time-series given by $\mathbf{H}_t$ is unique for every network.

C. Profile Assignment

The optimization algorithm along with dynamic time warping provides maximum load from load time-series and installed generation capacity in a 10 kV-0.4 kV network. Next every node in the 10 kV-0.4 kV network is assigned a load profile and/or a generation profile via the profile assignment process.

Every node in the 10 kV-0.4 kV network is assigned a value for its maximum load, which is an integer multiple of the minimum load value provided as a user defined input to DiNeMo while generating the distribution network topology.

Let a 10 kV-0.4 kV network have N nodes (0.4 kV and/or 10 kV), with the minimum load at any node being s_{min}. Maximum load at the nth node in the network is thus given by,

$$x_n = a_n s_{min} \quad \forall a_n \in \mathcal{Z}, n \in \{1, N\} \tag{9}$$

where a_n is an integer multiple for the nth node. The total maximum simultaneous load, according to DiNeMo, for a 10 kV-0.4 kV network is,

$$X = \sum_{n=1}^{N} x_n = s_{min} \sum_{n=i}^{N} a_n. \tag{10}$$

The optimization results indicate that the total maximum simultaneous load for a 10 kV-0.4 kV network is the sum of maximum loads for the load profiles $\mathbf{H}_t$, termed Y, as follows:

$$Y = \sum_{i=1}^{27} d_i \tag{11}$$

Let s'_{min} indicate a scaled minimum load at each node of the 10 kV-0.4 kV network, such that,

$$Y = s'_{min} \sum_{n=i}^{N} a_n = \sum_{n=1}^{N} y_n \tag{12}$$

$$y_n = a_n s'_{min} \quad \forall a_n \in \mathcal{Z}, n \in \{1, N\} \tag{13}$$

where, y_n is the scaled maximum load at the nth node. Thus, s'_{min} can be calculated from (10) and (12) as follows,

$$s'_{min} = s_{min} \frac{Y}{X}. \tag{14}$$

Assume that i^{th} load profile, $i \in \mathcal{L}$, is assigned to $k_i \in \mathcal{Z}$ nodes, in the 10 kV-0.4 kV network.

$$N = \sum_{i=1}^{27} k_i. \tag{}$$

Thus the maximum load for the ith load profile, denoted by d_i, is equally distributed amongst k_i nodes, which implies,

$$d_i = t_i k_i s'_{min} \tag{15}$$

where, t_i is an integer multiple assigned for i^{th} load profile. Therefore k_i can be calculated as follows,

$$k_i = round\left(\frac{d_i}{t_i s'_{min}}\right) \tag{16}$$

Notice that there are two unknowns in the above equation, t_i and k_i. A heuristics based approximation is used to determine the value of t_i, based on statistical information as follows.

The SLPs from SimBench are broadly classified into 7 levels of power consumption / maximum load. A similar classification is assumed for the time warped load time-series, $\mathbf{H}_t$. Let, c_i, denote the maximum load from a node which is assigned a load profile of the ith power consumption level. The consumption level for each load profile imposes a condition on maximum load for each load profile which will aid is assignment of the standard load profiles to the nodes.

$$c_{VII} \geq c_{VI} \geq c_V \geq c_{IV} \geq c_{III} \geq c_{II} \geq c_I \tag{17}$$

Note that the inequality (17) is not implemented as a hard constraint. Thus, from (15) and (17) the following condition can be accepted for the order of t_i,

$$t_{VII} \geq t_{VI} \geq t_V \geq t_{IV} \geq t_{III} \geq t_{II} \geq t_I. \tag{18}$$

The profile assignment starts from the nodes with maximum load according to DiNeMo by assigning a load profile with maximum power consumption level and progresses in a descending order of the maximum load. An appropriate value of k_i is chosen in accordance with the maximum demand from the load profile, d_i and an appropriate multiplying factor t_i. Finally, the maximum demand for the ith load profile is given as follows,

$$s_i = d_i / k_i \quad \forall i \in [1, 27] \tag{19}$$

In addition to load profiles, the aggregated PV and WPP generation capacities are assigned to appropriate nodes in the network. The following assumptions are considered while allocating the weather-dependent generation in the 10 kV-0.4 kV network:

- Minimum installed PV capacity: 1 kW
- PV generation can be installed at 0.4 kV or 10 kV nodes
- Minimum installed WPP capacity: 300 kW
- WPPs are installed only at 10 kV

- Installed generation at any consumer node is less than its maximum demand

Statistics for solar installations in the Danish grid, provided in [26], show that the self-consumption via PV generation is in the range of 20–30% for the residential sector and about 40% for the commercial sector, for the years in question. Residential PV plants, i.e. rooftop plants, have an installed capacity of 7 kW or less, in particular 3 kW PV installations being greatly preferred, while for the commercial sector, installed PV capacity is 7 kW or higher. Taking into account the statistics described in [26], the installed PV generation capacity is assumed to supply 25% of the maximum load for household loads, and 40% of the maximum load for commercial and agricultural loads. While assigning installed solar capacities to individual nodes, all of the above statistics are taken into account.

It is assumed that the minimum installed generation for a WPP is 300 kW connected only at the 10 kV nodes. In order to assign WPPs at the 10 kV node, wind installation statistics from [23] are used as a reference. For the geographical area of the 10 kV-0.4 kV networks, the maximum onshore wind installation is in the range of 3.6 MW-4 MW. However, a large number of WPPs have installed capacities of 1 MW. Hence, for assigning WPPs to the 10 kV nodes, a maximum to minimum approach is adopted. This implies that the total installed wind power generation in a 10 kV/0.4 kV network is divided into chunks of 3.6 MW WPPs and a remainder value if applicable, and assigned to the 10 kV nodes. If there are insufficient number of 10 kV nodes, then the total installed wind generation capacity is distributed amongst the available nodes.

The profile assignment exercise in each network is majorly a heuristic process based on the information about approximate load demand at each node (from DiNeMo) and statistical data for wind and solar PV installations. Location of particular load profiles, maximum load demands, and renewable energy generation assigned to each load affects the network operating characteristics on an hourly basis. However, on an aggregate level, the characteristics of each 10 kV-0.4 kV network remains intact.

IV. RESULTS

The optimization results are depicted and described for 10 kV–0.4 kV network at Bus 27 which serves as representative network for all the 10 kV-0.4 kV networks. A power flow analysis is also performed for this network.

A. Optimization Results

The optimization results, with and without DTW, for the 10 kV–0.4 kV networks at Bus 27, 28, and 46 are tabulated in Table II. It is observed that the root mean square error (RMSE) of the solution decreases with DTW, and the correlation of the solution with the aggregated load profile at 10 kV increases. However, there is a stronger decrease in the RMSE for networks at Buses 27 and 28 as compared to the network at Bus 46. This is because the network at Bus 46 is exceedingly dominated by RES, as will be shown in the following discussion. The optimization algorithm implicitly incorporates the generation profiles in the
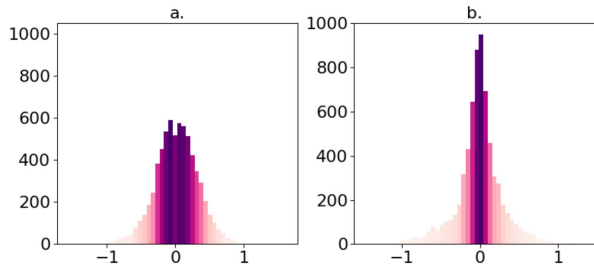
Fig. 5. **a.** Probability distribution for solution without DTW; **b.** Probability distribution for solution with DTW for network at Bus 27.
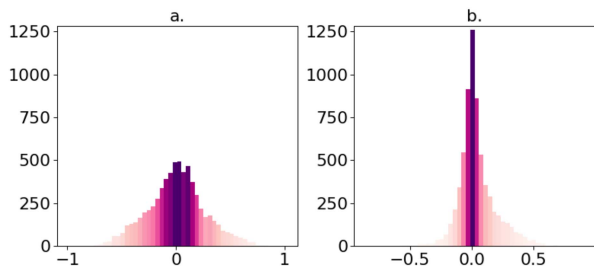

Fig. 6. **a.** Probability distribution for solution without DTW; **b.** Probability distribution for solution with DTW for network at Bus 28.

Fig. 7. Maximum demand for SLPs and total installed generation capacity for weather-dependent generation profiles.

optimization but the generation profiles are not subject to DTW (Refer to (5) and (7)).

The positive effect of performing DTW on the weighted sum of SLPs is most noticeable in the residual time-series. Figs. 5 and 6 captures the probability distribution of the solution without DTW and the solution with DTW for networks at Buses 27 and 28. After DTW, the solution time-series is more concentrated around *0* value compared to the solution without DTW. The 95th percentile value for the probability distribution of the preliminary solution is 0.523 and 0.48 while the 95th percentile for the probability distribution with DTW is 0.47 and 0.33 for network at Buses 27 and 28 respectively, which further suggests a reduction in the mismatch between the reference and the solution. DTW thus improves the correlation between the aggregated load time-series and the solution load time-series while also reducing the RMSE error. The increase in computation time due to DTW is minimal.

It is observed from Figs. 5 and 6 that, there is considerable error in the time-warped time-series as well. This implies that available SLPs, time-warped load profiles, and weather-dependent generation profiles fail to completely categorize the characteristic behavior of the aggregated load time series. The difference between the solution with DTW and the reference time-series is the residual time-series.

The final step in generating the Low Voltage (LV) network, shown in Fig. 2, is to distribute all the time-warped load time-series amongst individual 400 V or 10 kV nodes using the heuristic algorithm described in Section III-C.
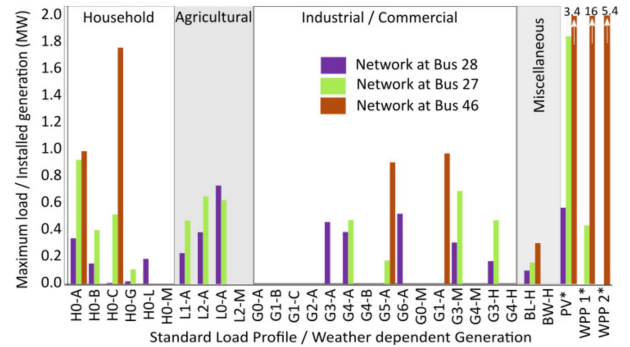
B. Network Models and Hourly Time-Series

The optimization algorithm specifies the maximum load from the standard load profiles and installed wind and PV generation in the network as depicted in Fig. 7. The x-axis in Fig. 7, except for Wind and PV, indicate the names of the SLPs as described in the SimBench dataset. Briefly, *H* represents the household SLPs, *L* represents agricultural SLPs, *G* represents industrial/commercial *slp*s, and the rest are miscellaneous. Note that not all the SLPs have non-zero values and the maximum demand from each profile differs for the three networks shown. It is also interesting to find that even though the aggregate load at 10 kV is positive, indicating a load only network, the optimization computes ≈ 1.85 MW of installed PV, and ≈ 0.44 MW of installed wind capacity which was un-observable in the aggregate load.

Table III presents key statistics for the loads connected to the networks at Bus 27, 28, and 46. The number of nodes in the networks suggests that Network at Bus 46 is the largest network amongst the three while Network at Bus 27 is the smallest. Population density of these geographical areas qualifies the networks at 27, 28, and 46 to be categorized as rural, semi-urban, and urban area networks. The categorization can also be drawn from the size of the network and the proportion of different load profiles. For eg. the network at Bus 46 has a dominant household load profile with no agricultural load. Given the size of this network, it qualifies to be categorized as a residential urban network.

A snapshot of the hourly time-series for 10 days for the network at Bus 27 and 46 is plotted in Figs. 8 and 9. The hourly time-series in Figs. 8 and 9 are broken down into broader load categories namely, household, agricultural, commercial/industrial, and miscellaneous. Amongst the dates shown in Fig. 8 7th, 8th, 14th, and 15th February fall on a weekend and a slight decrease in the industrial/commercial load profile is observable on those dates. This becomes more interesting for the load profile on the dates illustrated in Fig. 9 showing the dip in load demand from industrial/commercial loads over the new-years' holiday, and the following weekend on the 3rd and 4th January.

Figs. 10 and 11 plot the hourly generation from wind and PV for the same dates. Both the generation time-series depict
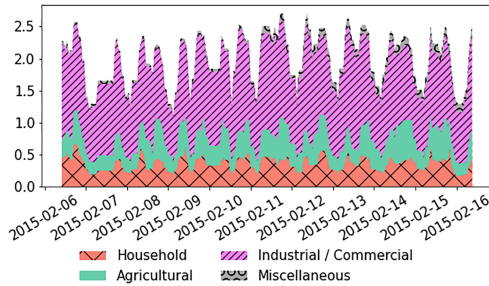
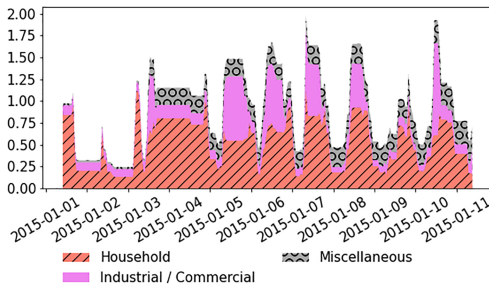Fig. 8. Stacked plot for hourly load time-series for Network at Bus 27.

Fig. 9. Stacked plot for hourly load time-series for Network at Bus 46.
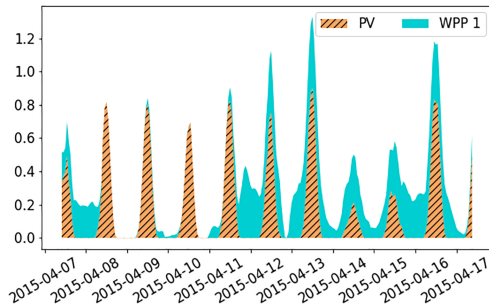

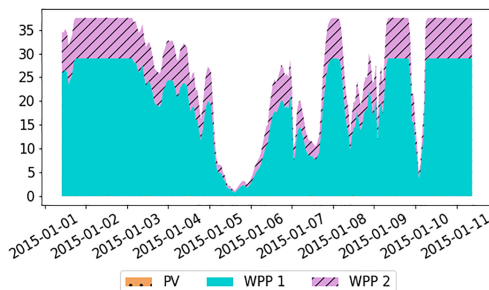Fig. 10. Hourly Solar and wind generation time-series for Network at Bus 27.

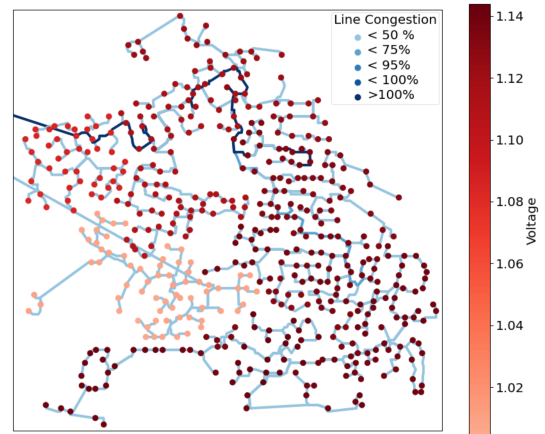Fig. 11. Hourly Solar and wind generation time-series for Network at Bus 46.

Fig. 12. Voltages and line congestion for one timestamp in the 10 kV-0.4 kV network connected at Bus 46 | Load: 1.39 MW | Generation: 17.667 MW | Line Losses: 1.96 MW.

C. Power Flow

The result of the power flow algorithm for one timestamp is provided in this section for the 10 kV-0.4 kV network at Bus 46. The power flow calculations are computed using Newton Rapson method in *PyPower*.

Key statistics for the network are tabulated in Table III. The network at Bus 46 is chosen because it contains a high share of weather-dependent renewable energy sources and it is one of the largest 10 kV-0.4 kV networks. A random timestamp is chosen to perform power flow to establish the plausibility of the load and generation time-series along with the 10 kV–0.4 kV networks. A Netwon Raphson AC power flow is run for the chosen timestamp. Note that the power flow is not optimized for this analysis and all tap-changers are set to nominal position.

The required load from the network at the 60 kV-10 kV sub-station is 1.4 MW. The total generation from the PV and WPPs installed in the network 10 kV-0.4 kV is 17.67 MW. The resulting voltages at all nodes and line loading in the 10 kV-0.4 kV network for this timestamp are pictorially represented in Fig.. Note that the nodes at the end of the distribution line experience higher voltages than the nodes closer to the 60 kV–10 kV substation. This is due to a high amount of distributed generation in the network. The total active power line loss in the network is 1.96 MW with maximum loss and maximum line loading observed in the distribution line connecting the network to the 60 kV-10 kV substation.

Similarly, a Newton Raphson AC power flow is run for all the entire DTU-ADN and it is found that the power flow converges at all timestamps.

V. SUMMARY

This paper proposes and presents the methodology used for the development of a multi-voltage active distribution network model, named DTU 7k-Bus Active Distribution Network (DTU-ADN). The DTU-ADN spans across 3 voltage levels, 60 kV-10 kV- 0.4 kV, and hosts an abundant amount of distributed renewable energy sources, primarily wind and solar power,

variations in renewable energy generation on a daily basis with a few days with minimum wind and solar power generation. Since the dates for Fig. 11 fall in the month of December, there is no PV generation observed, as the sunlight hours are limited and the PV production is hindered due to cloudy weather.

connected across all the voltage levels. The distribution network model is developed using a top-down approach, premised on the 60 kV distribution network model and correlations between load demand and wind and/or solar generation in a low voltage distribution network. The approach presented in this research expands the initial 60 kV network with 14 10 kV-0.4 kV networks at different 60 kV-10 kV substation nodes. Aggregated load (active and reactive power) and generation time-series, for a period of about 10 months, accompanying the 60 kV network, is used to assign load and generation profiles to the 10 kV–0.4 kV nodes.

The 60 kV network topology represents a real distribution network in Denmark while the 10 kV-0.4 kV networks are simulated from geographical data with the Distribution Network Modeling (DiNeMo) tool [19]. Measurement data is used to derive the aggregated load time-series at 60 kV nodes. The load profiles assigned to 10 kV and 0.4 kV nodes represent commercial/industrial, agricultural, household and miscellaneous loads. Finally, meteorological data is used to simulate wind and solar generation time-series using CorRES [21].

An optimization problem is formulated to calculate the aggregate proportion of the 27 standard load profiles along with wind and solar generation in one 10 kV-0.4 kV network. The objective of the optimization is to minimize the difference between the aggregated load profile at 60 kV–10 kV substation, and summation of the 27 standard load profiles with wind and solar generation. The optimization routine emerges with a preliminary result of a 10-20% difference between the aforementioned load profiles and a correlation of 0.6-0.9. Further on, the dynamic time warping method reduces the difference up to 5-15% with a correlation of 0.8-0.9. The difference in the dynamic time-warped time-series and the aggregated time series at 60 kV-10 kV substation is termed as the residual time-series and is also provided with the DTU-ADN data.

The aggregated 60 kV time-series data is derived from measurement data in Denmark, whereas, the standard load profiles from [20] originate from Germany. In addition, the load time series are also measured in different meteorological years, namely 2014-15 and 2016. A load time series represents the consumption pattern of consumers connected to the given network and is deeply subject to changes in the weather and temperature. This is one of the major intractable sources of difference between the optimized load profile and the aggregated 60 kV load profile. Although the wind and solar generation time series is simulated from meteorological data from the same geographical location as the 10 kV–0.4 kV networks, it does not consider expected or unexpected shut-downs or ramping down of the wind and solar power plants. Such shut-down or ramping down of the generated power may arise due to maintenance period or failure of the power plants, storm-shut downs, strategic ramp downs, etc. However, the aggregated load profile at the 60 kV-10 kV substation implicitly incorporates this information as it is derived from measurement data. Failure to account for the expected and unexpected decrease in generation adds another intractable source of difference in the optimization.

The 17 networks at 10 kV-0.4 kV epitomize different characteristic medium-low voltage distribution networks via different proportions of commercial, household, and agricultural profiles. Since the network topology are simulated from geographical data, they represent diversity in terms of the network topology, energy density, and can be grouped into urban, semi-urban, and rural networks. Wind and solar power produce from 2% to more than 300% of the total energy demand in different 10 kV-0.4 kV networks for the given period. Thus, the DTU-ADN houses 10 kV-0.4 kV networks with varying amounts of renewable energy penetrations.

The DTU-ADN provides an opportunity to study multi-voltage distribution networks with distinct characteristics and RES penetration levels. On one hand, the distribution networks can be employed to study, control, and optimize voltage profiles, line losses, network asset operation with high RES penetration. While on the other hand, the multi-voltage models can be used to promote active participation of distribution networks in the provision of flexibility services, through controllable power electronics-based distributed generation. The DTU-ADN also provides the adaptability to incorporate additional assets such as storage, electric vehicle charging, or analyze demand response in the distribution network.

REFERENCES

[1] R. A. Walling, R. Saint, R. C. Dugan, J. Burke, and L. A. Kojovic, "Summary of distributed resources impact on power delivery systems," *IEEE Trans. Power Del.*, vol. 23, no. 3, pp. 1636–1644, Jul. 2008.

[2] K. A. Alboaouh and S. Mohagheghi, "Impact of rooftop photovoltaics on the distribution system," *J. Renewable Energy*, vol. 2020, pp. 1–23, 2020.

[3] A. Baviskar, A. D. Hansen, K. Das, and M. Koivisto, "Challenges of future distribution systems with a large share of variable renewable energy sources – Review," in *Proc. 19th Wind Integr. Workshop*, 2020.

[4] K. Strunz, S. Barsali, and Z. Styczynski, "CIGRE task force C6.04.02: Developing benchmark models for integrating distributed energy re-sources," in *Proc. CIGRE 5th Southern Africa Regional Conf.: Study Committee C6 Colloquium*, vol. 6, no. Coll, 2005, pp. 4–5.

[5] K. Rudion, A. Orths, Z. A. Styczynski, and K. Strunz, "Design of benchmark of medium voltage distribution network for investigation of DG integration," in *Proc. IEEE Power Eng. Soc. Gen. Meeting*, 2006, Art. no. 6.

[6] K. Strunz *et al.*, "Benchmark systems for network integration of renewable and distributed energy resources, CIGRE Task Force C6.04.02, p. 119, 2014.

[7] K. P. Schneider *et al.*, "Analytic considerations and design basis for the IEEE distribution test feeders," *IEEE Trans. Power Syst.*, vol. 33, no. 3, pp. 3181–3188, May 2018.

[8] D. P. Chassin, K. Schneider, and C. Gerkensmeyer, "GridLAB-D: An open-source power systems modeling and simulation environment," in *Proc. Transmission Distrib. Expo. Conf. IEEE PES Powering Toward Future*, 2008, pp. 1–5.

[9] J. Amme, G. Pleßmann, J. Bühler, L. Hülk, E. Kötter, and P. Schwaegerl, "The eGo grid model: An open-source and open-data based synthetic medium-voltage grid model for distribution power supply systems," *J. Phys.: Conf. Ser.*, vol. 977, no. 1, 2018, Art. no. 012007.

[10] A. Navarro-Espinosa and L. Ochoa, "Dissemination document "Low voltage networks models and low carbon technology profiles"," *Ph.D. dissertation*, The University of Manchester, vol. 44, Jun. pp. 1–27, 2015.

[11] C. Matke, W. Medjroubi, and D. Kleinhans, "SciGRID - An open source reference model for the European transmission network (v0.2)," 2016. [Online]. Available: http://www.scigrid.de

[12] D. Montenegro, M. Hernandez, and G. A. Ramos, "Real time OpenDSS framework for distribution systems simulation and analysis," in *Proc. 6th IEEE/PES Transmiss. Distrib.: Latin America Conf. Expo.*, 2012, pp. 5–9.

[13] S. Meinecke *et al.*, "General planning and operational principles in german distribution systems used for simbench," in *Proc. 25th Int. Conf. Electric. Distrib.*, Jun. 2019, pp. 3–6. [Online]. Available: www.simbench.net

[14] A. Baviskar, A. D. Hansen, K. Das, and M. Koivisto, "DTU7k-bus active distribution network," 2021. [Online]. Available: https://doi.org/10.11583/DTU.c.5389910.v1

[15] S. Coast, "Open street maps," 2004. [Online]. Available: https://www.openstreetmap.org/

[16] D. Sarajlić and C. Rehtanz, "Low voltage benchmark distribution network models based on publicly available data," in *Proc. IEEE PES Innov. Smart Grid Technol. Europe*, 2019, pp. 1–5.

[17] S. Meinecke, N. Bornhorst, and M. Braun, "Power system benchmark generation methodology," in *Proc. NEIS 2018 - Conf. Sustain. Energy Supply and Energy Storage Syst.*, Feb. 2020, pp. 249–254.

[18] M. Sarstedt, G. Steffen, C. Blaufus, and L. Hofmann, "Modelling of Integrated Transmission and distribution grids based on synthetic distribution grid models," in *Proc. IEEE Milan PowerTech*, 2019, pp. 1–6.

[19] M. Grzanic, M. G. Flammini, and G. Prettico, "Distribution network model platform: A first case study," *Energies*, vol. 12, no. 21, 2019, Art. no. 4079.

[20] C. Spalthoff *et al.*, "SimBench: Open source time series of power load, storage and generation for the simulation of electrical distribution grids," in *ETG-Kongress 2019–Das Gesamtsystem im Fokusder Energiewende*, 2019, pp. 447–452.

[21] M. Koivisto *et al.*, "Using time series simulation tools for assessing the effects of variable renewable energy generation on power and energy systems," *Wiley Interdiscipl. Reviews: Energy Environ.*, vol. 8, no. 3, pp. 1–15, 2019.

[22] SOLARGIS, World Bank Group, and ESMAP, "Global solar atlas," 2020. [Online]. Available: https://globalsolaratlas.info/map?c=8.431621,-11.060486,8&r=SLE&s=7.885936,-11.18639&m=site

[23] P. G. Wang, M. Scharling, K. B. Wittchen, and C. Kern-Hansen, "2001–2010 dansk design reference year supplerende dataset: Projektrapport til energistyrelsen: Data til teknisk dimensionering for parametrene atmosfaeretryk, vindretning, skydaekke, vandtemperatur og jordtemperatur samt data til byggesagsbehan," Danmarks Meteorologiske Institut, 2013. [Online]. Available: https://ens.dk/

[24] H. Sakoe and S. Chiba, "Dynamic programming algorithm optimization for spoken word recognition," *IEEE Trans. Acoust., Speech, Signal Process.*, vol. 26, no. 1, pp. 43–49, Feb. 1978.

[25] L. Rabiner and B.-H. Juang, *Fundamentals of Speech Recognition*. Hoboken, NJ, USA: Prentice Hall, 1993.

[26] A. Peter, "National survey report of PV power applications in Denmark," PA Energy Ltd., Denmark, Tech. Rep., pp. 1–24, Aug. 2016. [Online]. Available: https://www.iea-pvps.org

Kaushik Das (Senior Member, IEEE) received the Ph.D. degree from the Technical University of Denmark (DTU), Lyngby, Denmark, in 2016. He is currently a Senior Researcher with the Department of Wind Energy, DTU. His research interests include hybrid power and energy plants, power system balancing, and grid integration of renewables in power systems. He is a Member of IEA Wind, CIGR, and other professional bodies. He is also a operating agent for IEA Wind Task 50 on Hybrid Wind Power Plant.

Matti Koivisto (Member, IEEE) received the M.Sc. and D.Sc. degrees from the School of Electrical Engineering, Aalto University, Espoo, Finland, in 2010 and 2016 respectively. He is currently a Researcher with the Department of Wind Energy, Technical University of Denmark, Lyngby, Denmark. His research interests include modeling large-scale wind and solar generations and their impacts on power and energy systems.

Aeishwarya Baviskar (Student Member, IEEE) received the M.Sc. degree in power engineering from the Technical University of Munich, Munich, Germany. She is currently working toward the Ph.D. degree with Department of Wind Energy, Technical University of Denmark, Lyngby, Denmark. Her research interests include power systems optimization, renewable energy sources, and their role in future power systems. Her current research focuses on optimization/control techniques for active distribution networks with a large share of renewable generation.

Anca Daniela Hansen (Member, IEEE) received the Ph.D. degree in modeling and control engineering from the Technical University of Denmark (DTU), Lyngby, Denmark. She is currently an Associate Professor with the Department of Wind Energy, DTU. She is the author or coauthor of more than 200 journal or conference papers, several research reports in her research fields, which include wind power integration and control including wind power plant modelling and control, ancillary services capabilities, provision and coordination from and between wind power plants operation.